Intermediate-band photovoltaic solar cell based on ZnTe:O

Weiming Wang,[a] Albert S. Lin, and Jamie D. Phillips
Department of Electrical Engineering and Computer Science, The University of Michigan, Ann Arbor, Michigan 48109-2122, USA

(Received 31 May 2009; accepted 9 June 2009; published online 6 July 2009)

Oxygen doping in ZnTe is applied to a junction diode in the aim of utilizing the associated electron states 0.5 eV below the bandedge as an intermediate band for photovoltaic solar cells. The ZnTe:O diodes confirm extended spectral response below the bandedge relative to undoped ZnTe diodes, and demonstrate a 100% increase in short circuit current, 15% decrease in open circuit voltage, and overall 50% increase in power conversion efficiency. Subbandgap excitation at 650 and 1550 nm confirms the response via a two-photon process and illustrates the proposed energy conversion mechanism for an intermediate band solar cell. © *2009 American Institute of Physics*.
[DOI: 10.1063/1.3166863]

The utilization of optical transitions at energies below the bandgap energy of semiconducting materials has been proposed for photovoltaic solar cells due to the potential of increased conversion efficiency in comparison to conventional devices operating on direct valence to conduction band optical transitions.[1–3] This approach, often termed intermediate- or impurity-band (IB) photovoltaics, provides a broad response to the solar spectrum via three optical transitions [valence to conduction, valence to intermediate, and intermediate to conduction band, Fig. 1(a)]. The provision of three optical transitions not only provides an increase in solar response but also reduces energy losses due to thermal relaxation of optically excited carriers. The intermediate band solar cell concept may be compared to the efficiency improvement for multijunction solar cells, where solar cell efficiency improvements are similarly gained by providing multiple absorption bands to maximize the response to the solar spectrum (maximize short circuit current) and minimize energy losses (maximize open circuit voltage). The intermediate-band approach offers the attractive prospect of achieving high efficiency in a more simplistic single-junction solar cell device. The theoretical conversion efficiency limit for intermediate band solar cells is predicted to be 63.2% with blackbody illumination[1] and 65.1% with AM1.5 spectrum,[4] comparable to the theoretical efficiency for optimized triple-junction solar cells with efficiencies of 63.8% and 67.0% under blackbody and AM1.5 illumination, respectively.[5]

Proposed approaches to realize intermediate band solar cells have included impurity doping,[6,7] quantum dots,[8–12] and dilute semiconductor alloys.[13–15] Impurity doping approaches have thus far not been successful due to nonradiative recombination channels associated with the impurities.[16] Quantum dots have demonstrated the intermediate band concept, where subbandgap response and increased efficiency have been reported.[17–19] The quantum dot systems used for IB solar cells thus far, however, have relatively shallow energy states relative to the optimal IB position at approximately 1/3 of the bandgap.[1,4] Furthermore, these systems have utilized GaAs as the host material, where the bandgap energy of 1.42 eV is significantly lower than the optimal bandgap for IB solar cells of 2.40 eV for 1 sun, and 1.95 eV for solar concentration of 10 000 under AM1.5 conditions.[4] Alternatively, dilute semiconductor alloys including InGaAsN (Ref. 13) and ZnTe:O (Refs. 15 and 20) have been proposed, where the intermediate band position is tunable with alloy composition. In these materials, properties may range from localized isoelectronic defect states at low concentration to the formation of an energy band at high concentration. These systems have reported optical properties that may be suitable for IB solar cells,[13,15–21] though reports of associated devices are lacking. In this work, the optical properties and photovoltaic response of ZnTe:O are presented.

ZnTe:O samples were grown by molecular beam epitaxy using solid source effusion cells for Zn and Te, and a rf plasma source for oxygen and nitrogen incorporation. Samples were grown on n^+-GaAs (100) substrates for material characterization and solar cell device structures. Nitrogen was used to achieve p-type ZnTe for the diode structure shown in Fig. 1(b). An oxygen flow rate of 1 SCCM (SCCM

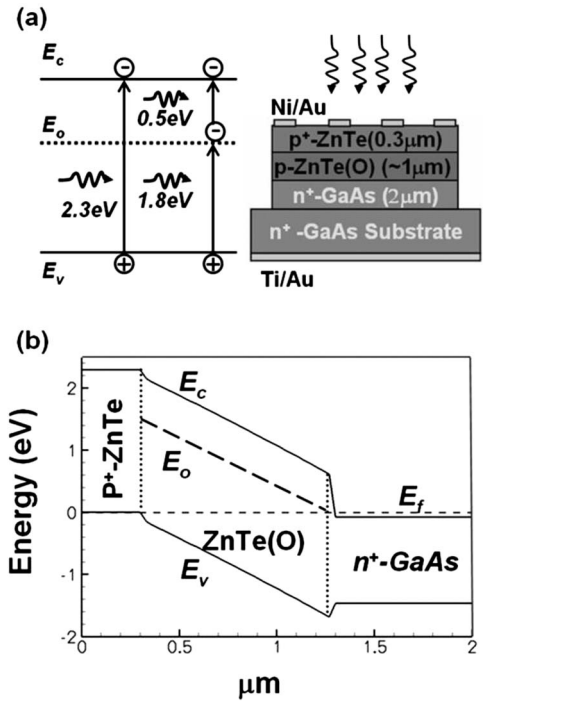

FIG. 1. Schematic of (a) optical transitions for ZnTe:O intermediate band solar cells and solar cell device structure incorporating ZnTe or ZnTe:O active regions, and (b) calculated band diagram of the p^+-ZnTe/ZnTe(O)/n^+-GaAs diode at thermal equilibrium.

[a]Electronic mail: umwmm@umich.edu.

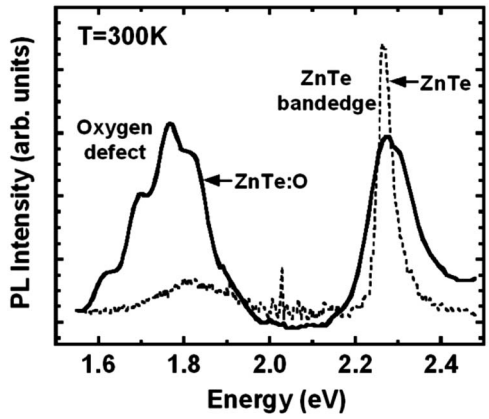

FIG. 2. Room-temperature photoluminescence spectra of ZnTe:O illustrating emission from both the ZnTe bandedge and oxygen related defect states.

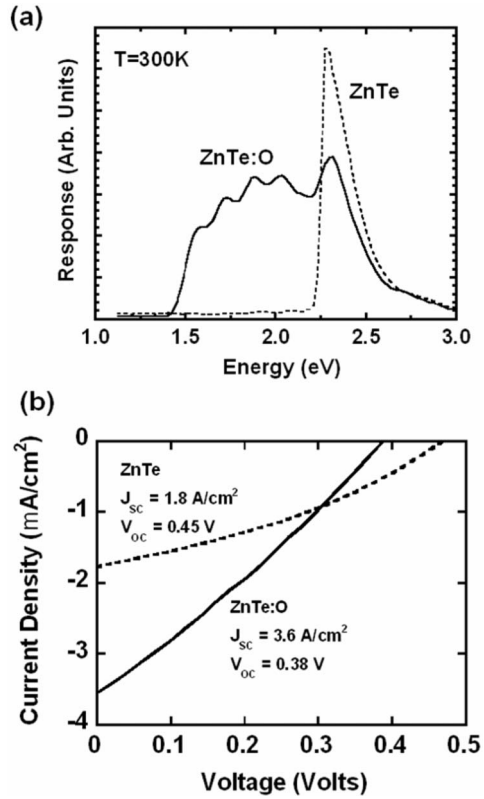

FIG. 3. Solar cell (a) spectral response and (b) current-voltage characteristics under AM1.5 conditions for ZnTe and ZnTe:O diodes.

denotes cubic centimeter per minute at STP) was used, where a concentration of 1×10^{19} cm^{-3} is estimated based on the assumption of a similar incorporation rate for oxygen and nitrogen. Photoluminescence measurements were taken using excitation from a HeCd 325 nm laser, a grating spectrometer, lock-in amplification, and a photodiode detector. Solar cell devices were fabricated using photolithography, metallization and liftoff, and wet chemical etching. Current-voltage characteristics were measured using a Keithley 4200 semiconductor parametric test system. Solar cell optical measurements were taken using a grating spectrometer for spectral response and a solar simulator for efficiency measurements.

A room-temperature photoluminescence spectrum for ZnTe:O grown on GaAs is shown in Fig. 2, indicating both a bandedge response for ZnTe at 2.3 eV and a strong sub-bandgap response related to oxygen doping in the range of 1.6–2.0 eV. In a majority of the ZnTe:O samples, the spectrum is dominated by defect emission, where the spectrum in Fig. 2 was chosen in order to illustrate both defect and ZnTe bandedge emission. In comparison, the photoluminescence spectrum for an undoped ZnTe sample shows a sharper bandedge transition and a much weaker defect emission. The presence of defect emission in the undoped ZnTe sample is believed to be due to residual oxygen present in the growth chamber. The strong radiative emission due to oxygen in ZnTe is consistent with previous detailed studies.[22] The strong emission for the oxygen defect in ZnTe denotes a highly radiative transition and is therefore a highly desirable characteristic for the IB solar cell. Complementary optical absorption spectra inferred from transmission measurements have been reported previously for samples deposited on sapphire under varying oxygen partial pressure.[23] A sharp bandedge response is observed for ZnTe without oxygen, while increasing sub-bandgap optical absorption is observed with increasing oxygen. The sub-bandgap optical absorption is consistent with the photoluminescence characteristics, and is similarly attributed to oxygen defects in ZnTe.

The spectral response for diodes fabricated with ZnTe and ZnTe:O absorber layers is shown in Fig. 3(a). For the case of the ZnTe diode, a sharp bandedge response is observed near 2.25 eV, with a gradual response decrease with increasing energy. The negligible response below the bandedge for the ZnTe diode indicates that the GaAs substrate does not contribute to the photocurrent, where the large band offsets block carrier transfer from *n*-GaAs to *p*-ZnTe. The response decrease at high energy is attributed to an increasing fraction of optical absorption in the heavily doped *p*-type ZnTe cap layer, where carrier collection will be impeded due to short carrier diffusion lengths in this layer. The ZnTe:O diode exhibits enhanced spectral response below the bandedge, where response is observed for energies down to 1.5 eV. It should be noted that the spectral response was obtained using monochromatic light and does not necessarily represent the true spectral response of a solar cell where a full spectrum is incident on the device. The monochromatic incidence does not provide a means of "pumping" carriers from the valence band to intermediate band in order to enable absorption from the intermediate to the conduction band.

The current-voltage characteristics for ZnTe and ZnTe:O solar cells are shown in Fig. 3(b) under AM1.5 illumination. A clear photovoltaic response is observed for both sets of devices, where an increased short circuit current density (J_{SC}) and reduced open circuit voltage (V_{OC}) are observed for the ZnTe:O, with an overall improvement of 50% in the power conversion efficiency. The increase in J_{SC} is approximately double and is consistent with the extended spectral response below the bandedge and corresponding larger number of photogenerated carriers. The source for the approximate 15% reduction in V_{OC} may be due to a number of factors, including increased nonradiative recombination and carrier occupation in the IB lowering the Fermi level position. The overall conversion efficiency of both devices are both relatively low (<1%), where significant development of materials growth and device structure are required to improve efficiency. Factors degrading conversion efficiency include high resistance, low shunt resistance of the junction, and small carrier lifetime associated with the junction tech-

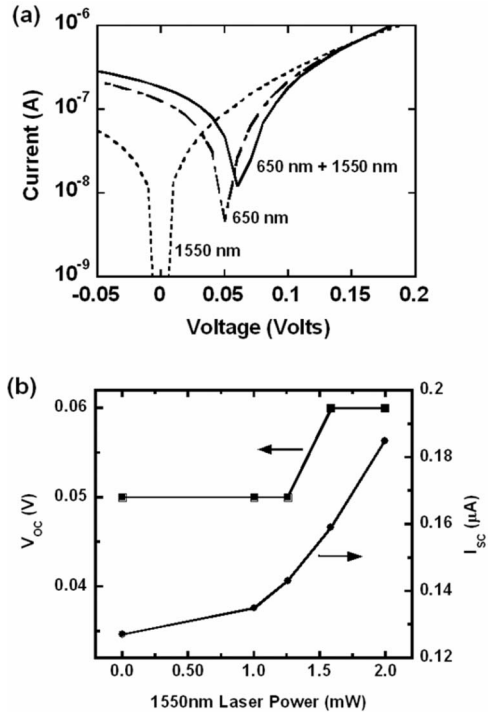

FIG. 4. Subbandgap response of a ZnTe:O solar cell with 0.09 cm^2 device area shown by (a) current-voltage characteristics under 1550, 650, and 650 nm+1550 nm excitation, and (b) I_{SC} and V_{OC} for variable 1550 nm laser excitation and constant 650 nm excitation.

nology and defects corresponding to the large lattice mismatch of the active region and GaAs substrate. Equivalent circuit modeling of the *I-V* characteristics provide values for the shunt resistance and series resistance of the devices, which were determined to be on the order of $R_{shunt}=3000\ \Omega\ cm^2$ and $R_{series}=300\ \Omega\ cm^2$. The value of series resistance is clearly a major limitation, where reduction to a more typical $R_{series}=1\ \Omega\ cm^2$ is estimated to provide a power conversion efficiency value of approximately 5% for the ZnTe:O device in Fig. 3. Further significant efficiency improvements are expected with the development of suitable buffer layers and ZnTe or II-VI based junction technologies to reduce defect density and associated nonradiative recombination.

The multiphoton process associated with intermediate-band transitions was further investigated using illumination by 650 nm (1.91 eV) and 1550 nm (0.8 eV) laser sources corresponding to energies below the ZnTe bandedge. The 650 nm laser provides energy necessary to excite an optical transition between the valence band and IB, while the 1550 nm laser provides the energy necessary to excite a transition from IB to conduction band. The ZnTe diodes did not exhibit any detectable response at these wavelengths. The ZnTe:O diodes do not show any detectable response for sole illumination at 1550 nm but do demonstrate significant response for illumination at 650 nm, consistent with the response observed at 1.91 eV in Fig. 3. The observed response for monochromatic 650 nm illumination suggests that carriers are excited into the IB and are subsequently promoted to the conduction band by further 650 nm photons, thermionic emission, or tunneling. Alternatively, it would be possible to extract carriers directly from the IB for the case where transport via IB states is significant. However, IB transport is unlikely in these experiments due to the low density of oxygen states and corresponding large spacing between neighboring oxygen atoms. The addition of 1550 to 650 nm illumination (simultaneous excitation) results in an increase in photocurrent and open circuit voltage. The photovoltaic response increases monotonically with increasing 1550 nm power density (Fig. 4), providing supporting evidence that the intended two-photon process for IB solar cells may be occurring in the ZnTe:O device. The nonlinear increase in the short circuit current with increasing 1550 nm illumination suggests that IB solar cell efficiency may be improved under higher excitation levels, indicating that these devices may further benefit from solar concentration.

In conclusion, ZnTe:O has been applied to diode structures exhibiting enhanced response to the solar spectrum in comparison to ZnTe due to photoexcitation below the bandgap energy. The increase in response for the ZnTe:O diodes translates to an approximate doubling of the short circuit current, while suffering an approximate 15% decrease in open circuit voltage. Subbandgap excitation experiments under 650 and 1550 nm excitation demonstrate the two-photon response characteristic desired for intermediate band solar cells and serve as a basis for further efforts to develop ZnTe:O and other dilute alloys or impurity materials for enhanced solar cell conversion efficiency.

Acknowledgment is made to the donors of the American Chemical Society Petroleum Research Fund for support of this research. The authors would like to thank Kuen-Ting Shiu for assistance with device measurements.

[1] A. Luque and A. Marti, Phys. Rev. Lett. **78**, 5014 (1997).
[2] A. Luque and A. Marti, Prog. Photovoltaics **9**, 73 (2001).
[3] W. Shockley and H. J. Queisser, J. Appl. Phys. **32**, 510 (1961).
[4] S. P. Bremner, M. Y. Levy, and C. B. Honsberg, Appl. Phys. Lett. **92**, 171110 (2008).
[5] A. Marti, and G. L. Araujo, Sol. Energy Mater. Sol. Cells **43**, 203 (1996).
[6] A. S. Brown and M. A. Green, J. Appl. Phys. **92**, 1329 (2002).
[7] G. Beaucarne, A. S. Brown, M. J. Keevers, R. Corkish, and M. A. Green, Prog. Photovoltaics **10**, 345 (2002).
[8] A. Marti, L. Cuadra, and A. Luque, IEEE Trans. Electron Devices **48**, 2394 (2001).
[9] V. Popescu, G. Bester, M. C. Hanna, A. G. Norman, and A. Zunger, Phys. Rev. B **78**, 205321 (2008).
[10] A. M. Kechiantz, L. M. Kocharyan, and H. M. Kechiyants, Nanotechnology **18**, 405401 (2007).
[11] G. Wei and S. Forrest, Nano Lett. **7**, 218 (2007).
[12] C. D. Cress, S. M. Hubbard, B. J. Landi, R. P. Raffaelle, and D. M. Wilt, Appl. Phys. Lett. **91**, 183108 (2007).
[13] K. M. Yu, W. Walukiewicz, J. W. Ager, D. Bour, R. Farshchi, O. D. Dubon, S. X. Li, I. D. Sharp, and E. E. Haller, Appl. Phys. Lett. **88**, 092110 (2006).
[14] E. Canovas, A. Marti, A. Luque, and W. Walukiewicz, Appl. Phys. Lett. **93**, 174109 (2008).
[15] K. M. Yu, W. Walukiewicz, J. Wu, W. Shan, J. W. Beeman, M. A. Scarpulla, O. D. Dubon, and P. Becla, Phys. Rev. Lett. **91**, 246403 (2003).
[16] P. Olsson, J.-F. Guillemoles, and C. Domain, J. Phys.: Condens. Matter **20**, 064226 (2008).
[17] A. Luque, A. Martí, N. López, E. Antolín, E. Cánovas, C. Stanley, C. Farmer, and P. Díaz, J. Appl. Phys. **99**, 094503 (2006).
[18] R. Oshima, Y. Shoji, A. Takata, and Y. Okad, J. Cryst. Growth **311** 1770 (2009).
[19] A. Martí, E. Antolin, C. R. Stanley, C. D. Farmer, N. Lopez, P. Diaz, E. Canovas, P. G. Linares, and A. Luque, Phys. Rev. Lett. **97**, 247701 (2006).
[20] A. S. Lin, W. Wang, and J. Phillips, J. Appl. Phys. **105**, 064512 (2009).
[21] Y. Nabetani, T. Okuno, K. Aoki, T. Kato, T. Matsumoto, and T. Hirai, Phys. Status Solidi A **203**, 2653 (2006).
[22] R. E. Dietz, D. G. Thomas, and J. J. Hopfield, Phys. Rev. Lett. **8**, 391 (1962).
[23] W. Wang, W. Bowen, S. Spanninga, S. Lin, and J. Phillips, J. Electron. Mater. **38**, 119 (2009).